Supporting Information

Harnessing the Power of Iridium AIEgens for NAD(P)H Detection in Aqueous Medium and Living Cells

Ajay Gupta,[a] Aryan Gautam,[a] Smaranika Patra,[a] Amit Kunwar,*[b,c] Pijus K. Sasmal*[a]

[a]School of Physical Sciences, Jawaharlal Nehru University, New Delhi 110067, India

[b]Radiation and Photochemistry Division, Bhaba Atomic Research Centre, Anushaktinagar, Mumbai 400085, India.

[c]Homi Bhabha National Institute, Anushaktinagar, Mumbai – 400094, India

**Corresponding authors: pijus@jnu.ac.in; pijussasmal@gmail.com (P. K. Sasmal) and kamit@barc.gov.in (A. Kunwar)*

Table of Contents

1. Materials

2. Instruments and Methods

3. Synthesis and Characterization

3.1 Synthesis

3.2 Purity of the probes

3.3 UV-visible spectra

3.4 Emission spectra and determination of quantum yield

3.5 Stability studies

3.6 Determination of lipophilicity

3.7 Determination of limit of detection of NADs

3.8 Characterization of NADs‑Ir(III) aggregates by DLS

3.9 Zeta (ξ) potential measurements

3.10 Selectivity of probe towards NAD(P)H in the presence of biologically relevant species

3.11 Cell viability assay

3.12 Imaging of NAD(P)H in live cells

3.13 Colocalization studies

Supplementary Schemes

Scheme S1 Schematic routes for the synthesis of probe **Ir1**.

Scheme S2 Molecular structures of the NAD species.

Supplementary Tables

Table S1 Physicochemical data of the iridium(III) probes (**Ir1** and **Ir2**).

Table S2 Limit of detection (LOD) of the probes with NADPH, $NADP^+$, NADH, and NAD^+.

Supplementary Figures

Fig. S1 ^1H NMR spectrum of compound **1** in $CDCl_3$.

Fig. S2-S3 ^1H NMR and ^{13}C NMR spectra of compound **2** in $CDCl_3$.

Fig. S4 ^1H NMR spectrum of **Ir1** in $CDCl_3$.

Fig. S5 ESI-HRMS spectrum of compound **1**.

Fig. S6 ESI-HRMS spectrum of compound **2**.

Fig. S7 ESI-HRMS spectrum of **Ir1**.

Fig. S8 HPLC chromatograms of **Ir1** and **Ir2**.

Fig. S9 Absorption and emission spectra of **Ir1** and **Ir2**.

Fig. S10 Emission decay curve for the probe **Ir1**.

Fig. S11 Stability of the probe **Ir1** in PBS.

Fig. S12-S13 Titration spectra of the probes upon addition of NAD species.

Fig. S14-S15 Size distribution histograms of **Ir1** and **Ir2** in the absence and presence of NAD species.

Fig. S16 The 3D electrostatic surface potential (ESP) distribution of $NADP^+$ and NADPH.

Fig. S17 Plot of cell viability by MTT assay of the probe **Ir1** in MCF7 cells.

Fig. S18 NAD(P)H imaging in non-cancer and cancer cells.

Supplementary References

1. Material

Solvents were distilled under argon from calcium hydride (CH_2Cl_2), magnesium chips (MeOH). Acetonitrile, diethyl ether, and dimethyl sulfoxide were used as dry HPLC grade solvents without further drying. All reactions were conducted under an argon atmosphere. 2-Phenylquinoline (PQ), 2,2′-bipyridine-4,4′-dicarboxylic acid, 1-(3-aminopropyl)imidazole, triethylamine (Et_3N), nicotinamide

adenine dinucleotide (NAD^+), nicotinamide adenine dinucleotide phosphate ($NADP^+$), reduced nicotinamide adenine dinucleotide (NADH) and its phosphorylated counterpart (NADPH) were purchased from Sigma-Aldrich. $IrCl_3 \cdot 3H_2O$ and potassium carbonate were obtained from Alfa-Aesar. Thionyl chloride, potassium hydroxide and methyl iodide were purchased from Central Drug House (CDH). Thin layer chromatography (TLC) was sourced from Merck, Germany. Dulbecco's modified Eagle medium (DMEM), Dulbecco's phosphate-buffered saline (PBS), trypsin, penicillin streptomycin solution (pen-strep), fetal bovine serum (FBS) and 3-(4, 5-dimethylthiazol-2-yl)-2, 5-diphenyltetrazolium bromide (MTT) were procured from Thermo Fischer Scientific. Hoechst 33342 were sourced from Invitrogen. MCF7 cells were obtained from the Cell Repository at National Centre for Cell Science (NCCS), Pune. Double distilled water and Milli-Q water (~18.8 mΩ.cm resistivity) (CDUFBI001, Millipore, USA) were used for the preparation of all the aqueous solutions. Iridium dimer ($[Ir(PQ)_2Cl]_2$) was synthesized as reported in the literature.[1] The probe **Ir2** was prepared according to the literature report.[2] The purity of the synthesized iridium(III) probes (**Ir1** and **Ir2**) was determined to be ≥ 95% based on NMR, high-resolution MS, and RP-HPLC.

2. Instruments and Methods

TLC analysis was performed on aluminium plates coated with silica gel containing a fluorescent indicator. Ligands and probes were purified using 60-120 mesh silica gel column chromatography. ^1H and ^{13}C NMR spectra were acquired on Bruker 500 MHz spectrometer in $CDCl_3$ and DMSO-d_6 at ambient temperature, with tetramethylsilane (TMS) as the internal standard. NMR standards used were as follows: (^1H-NMR) $CDCl_3$ = 7.26 ppm; DMSO-d_6 = 2.50 ppm. (^{13}C-NMR) $CDCl_3$ = 77.00 ppm; DMSO-d_6 = 39.52 ppm. All chemical shifts (δ) are reported in ppm relative to TMS. Spin multiplicities were reported as a singlet (s), doublet (d), triplet (t), doublet of doublets (dd), multiplet (m) and broad (br) with coupling constant (J) reported in Hz. Electrospray ionization high resolution mass spectra (ESI-HRMS) were obtained using a Waters make ESI-MS model synapt G2 high-definition mass spectrometry. Fourier transform-Infrared (FT-IR) spectra were recorded using IR Affinity-1S (Shimadzu, Kyoto, Japan) FT-IR spectrophotometer equipped with a single reflection attenuated total reflectance (ATR) accessory. The spectra were measured in the range of 4000 to 450 cm^{-1} with a resolution of 4 cm^{-1} and 45 scans. In the IR spectra, peak (band) shapes and signal intensities (height) are denoted using following abbreviations: br = broad, vs = very strong, s = strong, m = medium and w = weak. The purity of probes was determined by analytical HPLC system (Thermo Scientific Dionex Ultimate 3000) equipped with UV-Vis detector using reversed-phase C18 column (Acclaim, Length 250 mm, internal dia. 4.6 mm, particle size 5 μm, pore size 120 Å) operating at room temperature (RT). Absorption and emission spectra, and quantum yields were recorded using a SpectraMax M2 plate reader (Molecular Devices) and an Edinburgh Instruments F900 fluorescence spectrophotometer. Dynamic light scattering (DLS) measurements were performed using a Zetasizer Nano ZS90 (Malvern

Instrument Ltd., Worcestershire, UK). All luminescence measurements were conducted under aerated conditions.

3. Synthesis and Characterization

3.1 Synthesis

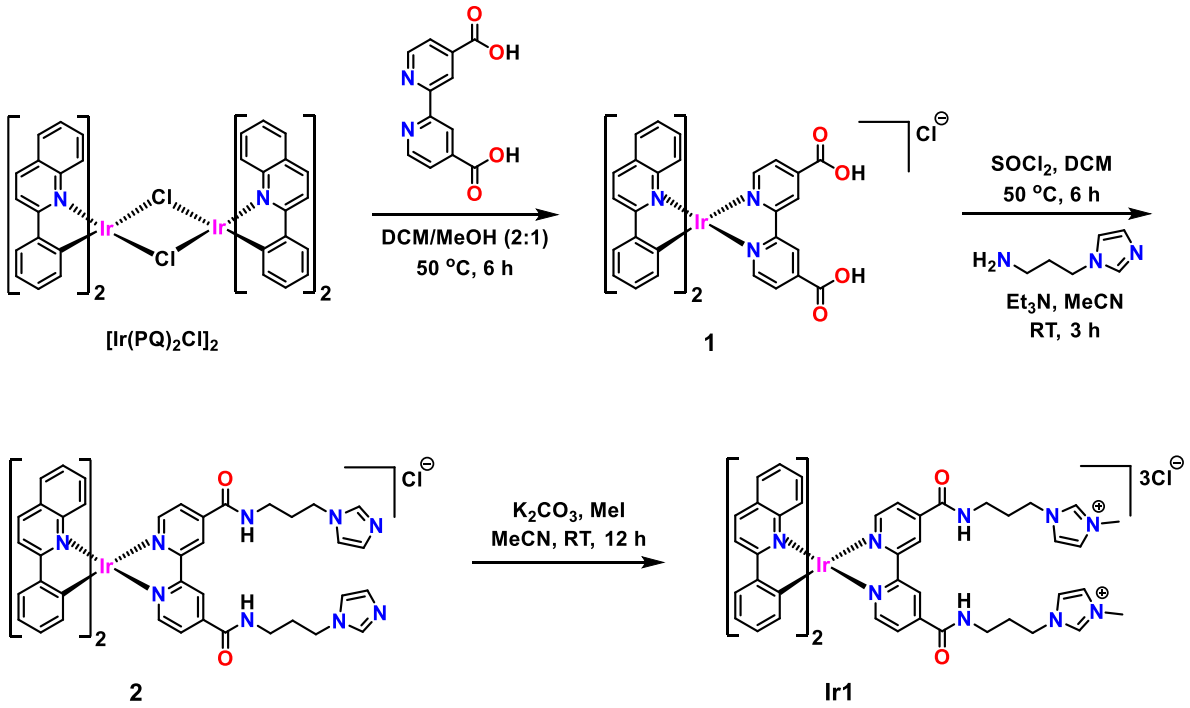

Scheme S1 Schematic routes for the synthesis of probe **Ir1**. Here, PQ = 2-phenylquinoline.

Synthesis of compound 1

The Ir(III) dimer ($[Ir(PQ)_2Cl]_2$, 30 mg, 0.023 mmol) and 2,2′-bipyridine-4,4′-dicarboxylic acid (12.7 mg, 0.051 mmol) were placed in an oven-dried round bottom-flask sealed with a rubber septum under argon atmosphere. Degassed CH_2Cl_2/MeOH (1.5 mL; 2:1 v/v) was then added. The reaction mixture was heated to 50 °C and stirred for 6 h. After cooling to room temperature, the solvent was removed using a rotary evaporator. The resulting solid was washed with diethyl ether (3 x 10 mL) and purified by silica gel column chromatography using CH_2Cl_2/MeOH (20:1, v/v) as the eluent. The purified product was dried under vacuum, yielding an orange-red powder **1** (Yield: 40 mg, 98%).

^{1}H-NMR (500 MHz, $CDCl_3$): δ (ppm) 8.50 (dd, J = 11.7, 8.8 Hz, 4H), 8.43 (s, 2H), 8.25 (d, J = 7.9 Hz, 2H), 8.06 (d, J = 5.5 Hz, 2H), 7.87 (d, J = 8.0 Hz, 2H), 7.81 (d, J = 5.4 Hz, 2H), 7.37 (t, J = 7.5 Hz, 2H), 7.29 (d, J = 8.9 Hz, 2H), 7.14 (t, J = 7.4 Hz, 2H), 7.05 (t, J = 7.8 Hz, 2H), 6.80 (t, J = 7.4 Hz, 2H), 6.42 (d, J = 7.6 Hz, 2H). ESI-HRMS (m/z) calculated for $C_{42}H_{28}IrN_4O_4^+$ $[M]^+$: 845.1734, found: 845.1730.

Synthesis of compound 2

Compound **1** (40 mg, 0.045 mmol) was dissolved in dry DCM (2.5 mL), and thionyl chloride (800 µL, 11.0 mmol) was added dropwise over 10 min. The reaction mixture was refluxed under an argon atmosphere for 6 h. After cooling to room temperature, the excess solvent was removed under high vacuum pump, yielding a red oily residue, which was then dissolved in MeCN (1 mL). A solution of 1-(3-aminopropyl)imidazole (27 µL, 0.227 mmol) and triethylamine (60 µL, 0.440 mmol) in MeCN (1 mL) was added dropwise over 10 min to the acid chloride solution. The reaction mixture was stirred at room temperature for 3 h, after which the solvent was removed under high vacuum. The resulting oily residue was washed with diethyl ether (3 x 10 mL) to obtain a powder. This powder was dissolved in DCM (20 mL) and washed sequentially with a 5% $NaHSO_4$ solution (3 x 10 mL) and brine (1 x 20 mL). The organic phase was dried over Na_2SO_4, and the solvent was evaporated to yield a red powder (Yield: 47 mg, 99%).

^{1}H-NMR (500 MHz, $CDCl_3$): δ (ppm) 9.89 (s, 2H), 9.41 (s, 2H), 8.48 (s, 1H), 8.21 (m, 4H), 8.15 (d, *J* = 8.4 Hz, 2H), 8.01 (m, 5H), 7.69 (d, *J* = 7.6 Hz, 2H), 7.35 (t, *J* = 7.3 Hz, 2H), 7.16 (m, 7H), 7.09 (s, 1H), 6.96 (t, *J* = 7.5 Hz, 2H), 6.81 (t, *J* = 7.1 Hz, 2H), 6.51 (d, *J* = 7.3 Hz, 2H), 4.21 (m, 4H), 3.44 (t, *J* = 4.3 Hz, 4H), 2.21 (m, 4H). ^{13}C-NMR (125 MHz, $CDCl_3$): δ (ppm) 169.74, 162.53, 156.36, 150.05, 147.89, 147.31, 145.31, 142.96, 140.26, 134.76, 131.55, 131.20, 129.25, 127.57, 127.16, 127.05, 126.83, 126.79, 124.53, 123.44, 123.42, 122.28, 117.47, 65.91, 54.81, 30.15. ESI-HRMS (*m/z*) calculated for $C_{54}H_{46}IrN_{10}O_2^+$ $[M]^+$: 1059.3429, found: 1059.3415.

Synthesis of Ir1

A suspension of K_2CO_3 (20.4 mg, 0.146 mmol) in dry MeCN (1 mL) was added to a solution of compound **2** (25 mg, 0.022 mmol) and stirred under an argon atmosphere for 1 h. The reaction mixture was filtered and removed insoluble K_2CO_3, and the filtrate was dried using a rotary evaporator. The resulting solid was re-dissolved in dry MeCN (1 mL), followed by the addition of methyl iodide (3.2 µL, 0.050 mmol). The solution was stirred at room temperature for 12 h under an argon atmosphere. The solvent and excess methyl iodide were removed using a rotary evaporator. The residue was dissolved in dry MeCN (500 µL), and a saturated solution of NH_4Cl (500 µL) was added, followed by stirring at room temperature for 1 h. After the removal of the solvent by rotary evaporation, a white-red solid was obtained. The solid was dissolved in DCM (2 mL) and filtered to remove insoluble NH_4Cl. The filtrate was dried using a rotary evaporator, yielding a red-orange solid product. Yield: 19 mg, 72%.

^{1}H-NMR (500 MHz, $CDCl_3$): δ (ppm) 9.86 (s, 1H), 9.51 (m, 2H), 9.02 (d, *J* = 4.4 Hz, 1H), 8.24 (dd, *J* = 11.0, 7.0 Hz, 5H), 8.16 (d, *J* = 8.6 Hz, 2H), 8.00 (d, *J* = 6.3 Hz, 4H), 7.70 (m, 4H), 7.46 (s, 1H), 7.37 (t, *J* = 7.0 Hz, 2H), 7.21 (d, *J* = 8.9 Hz, 2H), 7.16 (t, *J* = 7.2 Hz, 2H), 7.09 (t, *J* = 7.8 Hz, 2H), 6.82 (t, *J* = 7.2 Hz, 2H), 6.49 (d, *J* = 7.5 Hz, 2H), 4.50 (t, *J* = 6.3 Hz, 4H), 4.03 (s, 6H), 3.56 (m, 4H), 2.33 (m, 4H). ESI-HRMS (*m/z*) calculated for $C_{56}H_{52}IrN_{10}O_2^{3+}$ $[M]^{3+}$: 363.1296, found: 363.1297.

3.2 Purity of the probes

The purity of the probes was assessed using reverse-phase HPLC (RP-HPLC). A 20 μL solution of the probes (50 μM) in H_2O/acetonitrile (80/20, v/v) was injected into a RP-HPLC column. The detection wavelength was set at 254 nm. HPLC-grade acetonitrile (MeCN) and Millipore water containing 0.1% TFA (v/v) were used as the mobile phase. The gradient was adjusted from 95% water and 5% MeCN to 50% water and 50% MeCN over 30 min, with a flow rate of 1 mL min^{-1}.

3.3 UV-visible spectra

The absorption spectra of the probes (**Ir1** and **Ir2**) were recorded in water containing 0.2% DMSO at room temperature. All UV-vis spectroscopic measurements were performed using quartz cuvettes with 10 mm optical path length, and wavelengths were reported in nanometers (nm).

3.4 Emission spectra and determination of quantum yield

The emission spectra of probes were recorded in water containing 1% DMSO at room temperature using a quartz cuvette with a 10 mm optical path length. The probes were excited at 425 nm. Quantum yields (Φ) were measured in MeCN at room temperature, using $[Ru(bpy)_3](PF_6)_2$ (Φ = 0.0504) as a reference.

3.5 Stability studies

The stability of probe **Ir1** was evaluated using UV-vis spectroscopy in PBS at pH 7.4. Briefly, **Ir1** (20 μM) was dissolved in PBS (10 mM, pH 7.4) containing 0.4 % DMSO and analyzed by UV-vis spectroscopy at room temperature at different time points up to 24 h.

3.6 Determination of lipophilicity

The lipophilicity (log $P_{o/w}$) of the probes was determined using the classical flask-shaking method.[3] Briefly, 0.5 mg of each probe was added to 3 mL of a 1:1 (v/v) mixture of n-octanol and water and vigorously mixed for 24 h. The mixture was then allowed to stand for an additional 24 h to reach equilibrium. After phase separation, the concentration of the probes in the n-octanol (C_o) and water (C_w) phases were determined using UV-vis spectroscopy to calculate log $P_{o/w}$ = log $[C]_o/[C]_w$ values.

3.7 Determination of limit of detection (LOD) of NADs

A solution of probes **Ir1** and **Ir2** (50 μM) was prepared in water containing 1% DMSO, with a total volume of 2 ml. The probes were then titrated with NAD species (NADPH, $NADP^+$, NADH, and NAD^+) at room temperature, and their emission spectra were recorded 1 min after each addition. A plot of the emission intensity at the emission maxima as a function of NADs concentration showed a linear dynamic response. The limit of detection (LOD) of NADs using the probes was calculated using the following formula:[4]

$$LOD = 3\sigma/S$$

where σ is the standard deviation (SD) obtained from six independent measurements of the emission intensity of the probes in aqueous media without any NAD species, and S is the slope obtained from the linear fitting of the titration curves.

3.8 Characterization of NADs⁻Ir(III) aggregates by DLS

The hydrodynamic diameters (d) of **Ir1** and **Ir2** and NADs−Ir(III) aggregates were determined using dynamic light scattering (DLS). For this, an aqueous solution of 50 μM probe, with or without 3 μM of NADs, was prepared in a total volume of 2 mL containing 1% (v/v) DMSO in water. DLS measurements were conducted at 25 ℃ using a 4 mW laser with a wavelength of 632.8 nm and a detector angle at 90º.

3.9 Zeta (ξ) potential measurements

The zeta potential of probe **Ir1** (50 μM) with and without 3 μM NADs, was measured at 25 ºC in a 1 mL cuvette containing 1% (v/v) DMSO in water. A voltage of 100 V was applied during the measurements.

3.10 Selectivity of probe towards NAD(P)H in the presence of biologically relevant species

The selectivity of **Ir1** (50 μM) towards NAD(P)H (6 μM) was studied in 1% (v/v) DMSO in water, with a total volume of 200 μL, in the presence of biologically competing species at room temperature. Selectivity was assessed by measuring the emission intensity of **Ir1** using a SpectraMax® M2e fluorescence microplate reader (Molecular Devices LLC, USA). Measurements were performed in 96 well plates with an excitation wavelength of 425 nm, a 660 nm cut-off filter, and an emission wavelength of 690 nm. The concentrations of cationic salts, including NaCl (Na^+), KCl (K^+), $CaCl_2$ (Ca^{2+}), $MgCl_2$ (Mg^{2+}), $FeCl_3$ (Fe^{3+}), $ZnCl_2$ (Zn^{2+}) were used at 100 μM. Whereas, the concentrations of competing molecules, such as sodium acetate (NaOAc), sodium dihydrogen phosphate (NaH_2PO_4), glycine (Gly), lysine (Lys), methionine (Met), cysteine (Cys), tyrosine (Tyr), glucose, glutathione (GSH), adenosine diphosphate (ADP), adenosine triphosphate (ATP), nicotinamide adenine dinucleotide (NAD^+), nicotinamide adenine dinucleotide phosphate ($NADP^+$) were kept at 10 μM except calf-thymus DNA (ct-DNA) that was 2 mg/L.

3.11 Cell viability assay

The cytotoxicity of the probe **Ir1** was accessed using the MTT assay. Stock solutions of probe **Ir1** was prepared in DMSO. Cultured cells were seeded in 96 well plates in penta-triplicate at a density of 5,000 cells per well. After 24 h of incubation, the media were removed, and the cells were treated with each compound at eight increasing concentrations, diluted in culture media containing <1% DMSO. The total media volume in each well was maintained at 200 μL. Cells were incubated with the probe for 24 h, after which the media were replaced with 200 μL of incomplete media containing MTT (0.5 mg mL^{-1} in PBS) and further incubated at 37 °C for 4 h. The media were then replaced with 200 μL of DMSO to dissolve the formed formazan crystals, followed by incubation at room temperature for 15 min. Absorbance was measured at 570 nm using a SpectraMax spectrometer (Molecular Devices), and the data obtained were analyzed using Origin 18.

3.12 Imaging of NAD(P)H in live cells

All experiments were performed in live cells to avoid artifacts associated with fixation procedures. Four sets of experiments were conducted using MCF7 cells. For this, cells were seeded on coverslips at a density of 10^5 cells per well 24 h prior to the experiments. In the first set, cells were treated with **Ir1** (10 μM) for 30 min. In the second and third sets, cells were incubated with 10 and 20 mM glucose, for 30 min, respectively, followed by treatment with **Ir1** (10 μM) for an additional 30 min before imaging. In the fourth set, cells were incubated with 5 mM pyruvate for 30 min prior to the addition of **Ir1** (10 μM) for 30 min. Cells were imaged using a Nikon Eclipse Ti-E microscope following the respective treatments.

3.13 Colocalization studies

The intracellular localization of **Ir1** was investigated using confocal microscopy. For this, MCF7 cells were seeded on coverslips at a density of 10^5 cells per well 24 h prior to the experiment. The cells were then treated with the probe **Ir1** (10 μM) for 1 h in DMEM complete media. Following treatment, the cells were washed with 1X PBS and simultaneously stained with MitoTracker Green FM (150 nM) and Hoechst (1 μM) for 30 min. The media were then removed, and the cells were thoroughly washed with PBS (4 x 1 mL) before microscopy imaging. The stained cells were visualized under a Nikon Eclipse Ti-E microscope. Hoechst and **Ir1** were both excited with a 405 nm laser. Hoechst emission was recorded in channel 1 with a bandpass filter range of 450/50 nm, while **Ir1** emission was recorded in channel 3 with a long pass filter range of 595/50 nm. MitoTracker Green emission was captured in channel 2 using a bandpass filter range of 540/30 nm. The obtained images were analysed using Fiji software (NIH), and the extent of co-localization was determined using scatter plot with Pearson's correlation coefficient (PCC).

Table S1 Physicochemical data of the cyclometalated iridium(III) probes (**Ir1** and **Ir2**).

Probes	λ_{abs}[a]/nm ($\varepsilon/10^3$ M^{-1} cm^{-1})	λ_{em}[a]/nm	Φ[b]	τ/ns[c]	log $P_{o/w}$[d]
Ir1	276 (23.4), 314 (12.5), 346 sh (9.5), 430 (2.6)	692	0.077	96	0.94
Ir2	258 (48.4), 276 (48.5), 314 (27.3), 350 sh (19.9), 428 (5.9)	680	0.094	65	1.82

[a]Absorption (λ_{abs}) and emission (λ_{em}) spectra were recorded in water with 0.2% and 1% DMSO, respectively. The emission spectra were recorded upon excitation at 425 nm. [b]Quantum yields (Φ) were determined in MeCN using $[Ru(bpy)_3](PF_6)_2$ (Φ = 0.0504) as the reference. [c]The lifetimes (τ) were measured in MeCN at room temperature at the emission maxima. [d]Lipophilicity (log $P_{o/w}$) values obtained by determining the partition coefficient of the probes in n-octanol/water.

Table S2 The limit of detection (LOD) of the probes **Ir1** and **Ir2** towards NADs.

Probes	NADPH	$NADP^+$	NADH	NAD^+
Ir1	22 nM	124 nM	20 nM	170 nM
Ir2	540 nM	330 nM	760 nM	500 nM

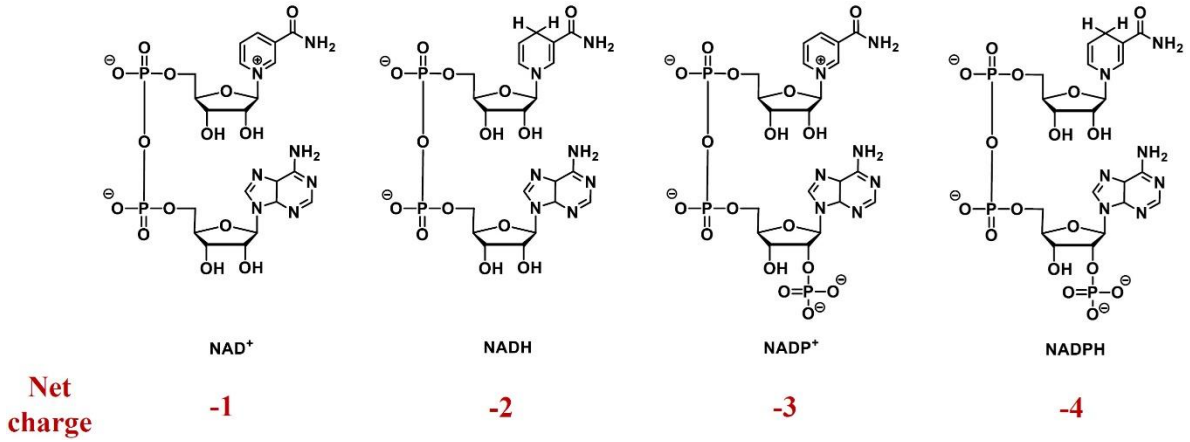

Scheme S2 Molecular structures of the NAD species showing the net charges.

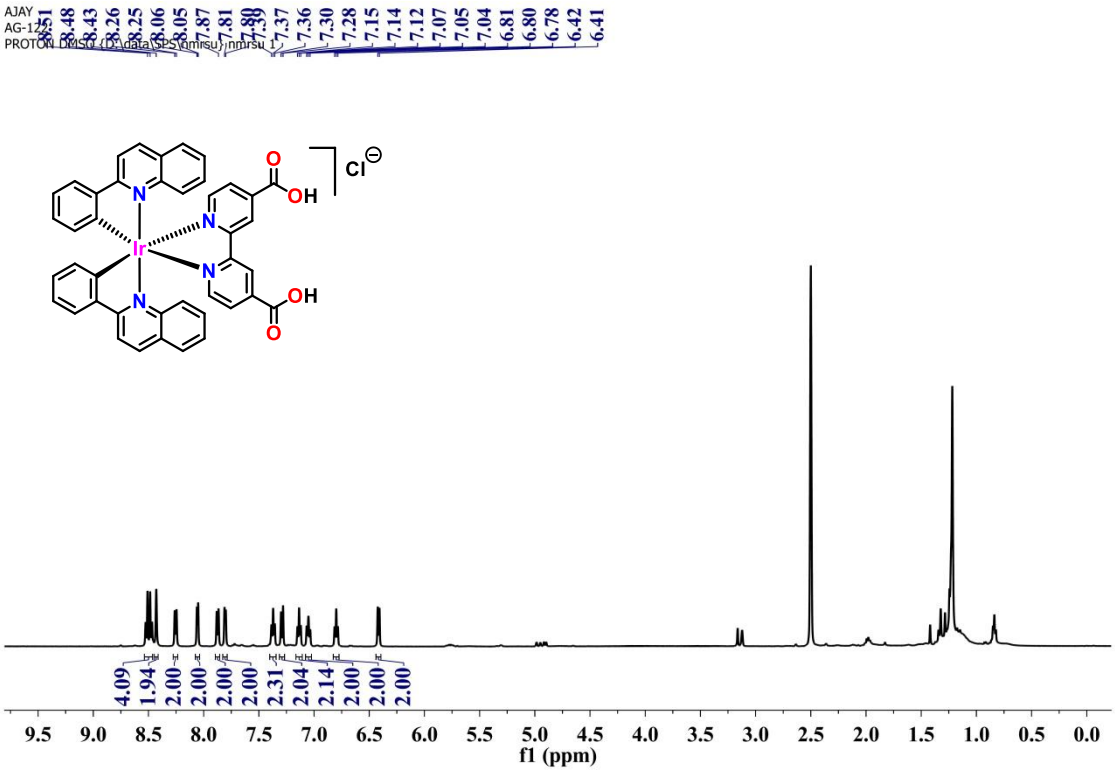

Fig. S1 ^{1}H-NMR spectrum of compound **1** in DMSO-d_6 at 298K.

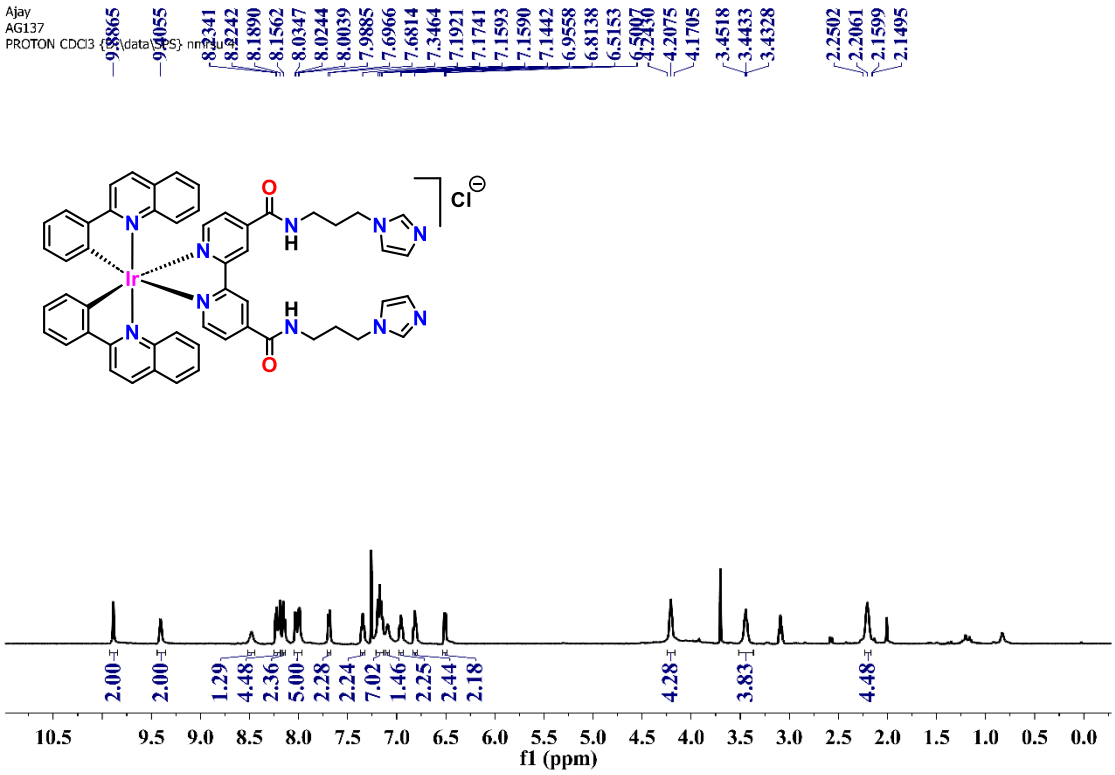

Fig. S2 ^{1}H-NMR spectrum of compound **2** in $CDCl_3$ at 298K.

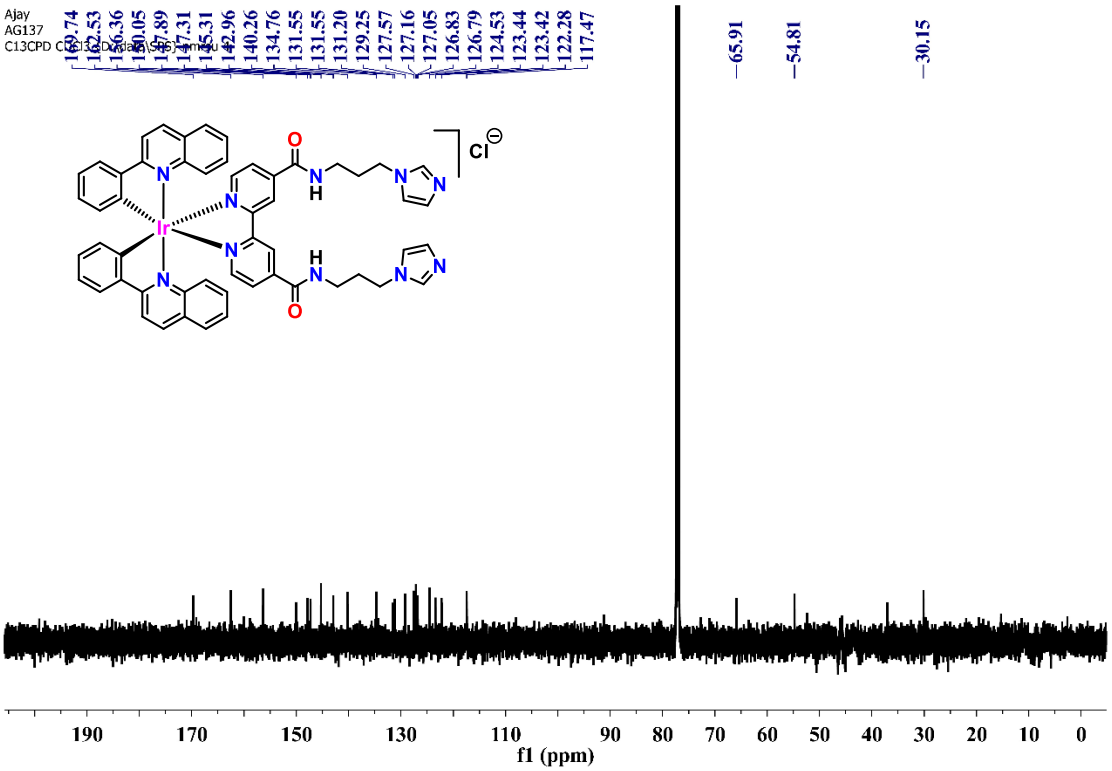

Fig. S3 ^{13}C-NMR spectrum of compound **2** in $CDCl_3$ at 298K.

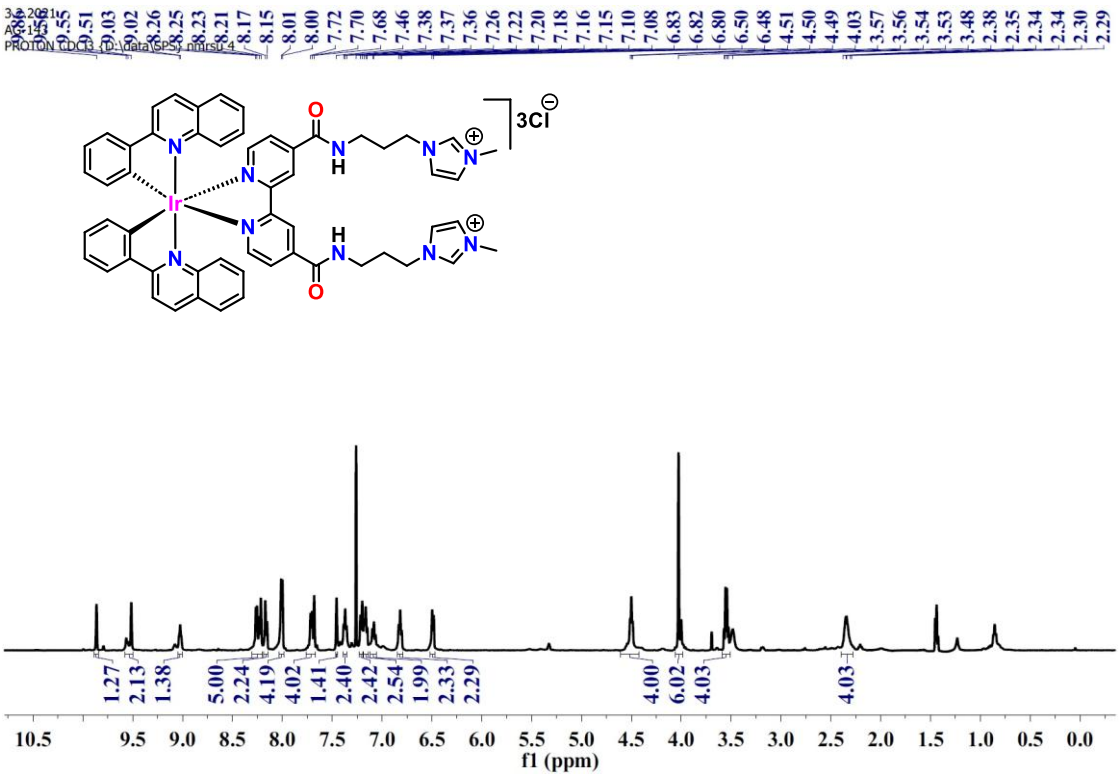

Fig. S4 ^{1}H-NMR spectrum of **Ir1** in $CDCl_3$ at 298K.

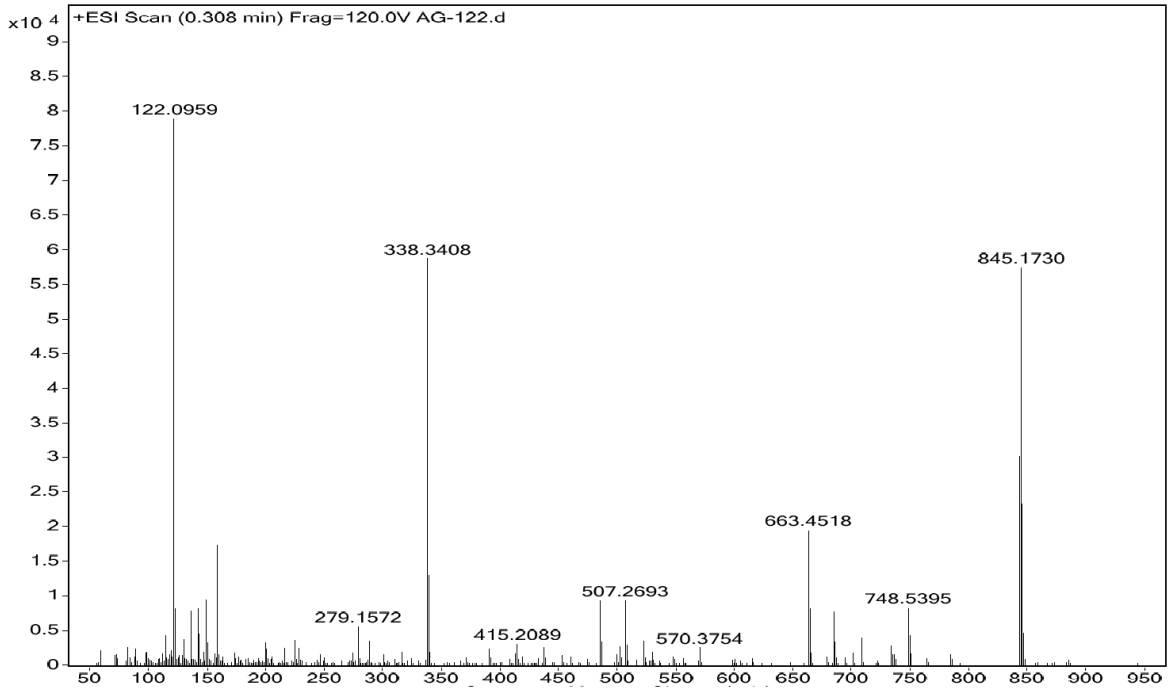

Fig. S5 Mass spectrum of **1** in DCM/MeOH showing the peak at 845.1730 (*m/z*) assignable to $[M]^+$ at 298K.

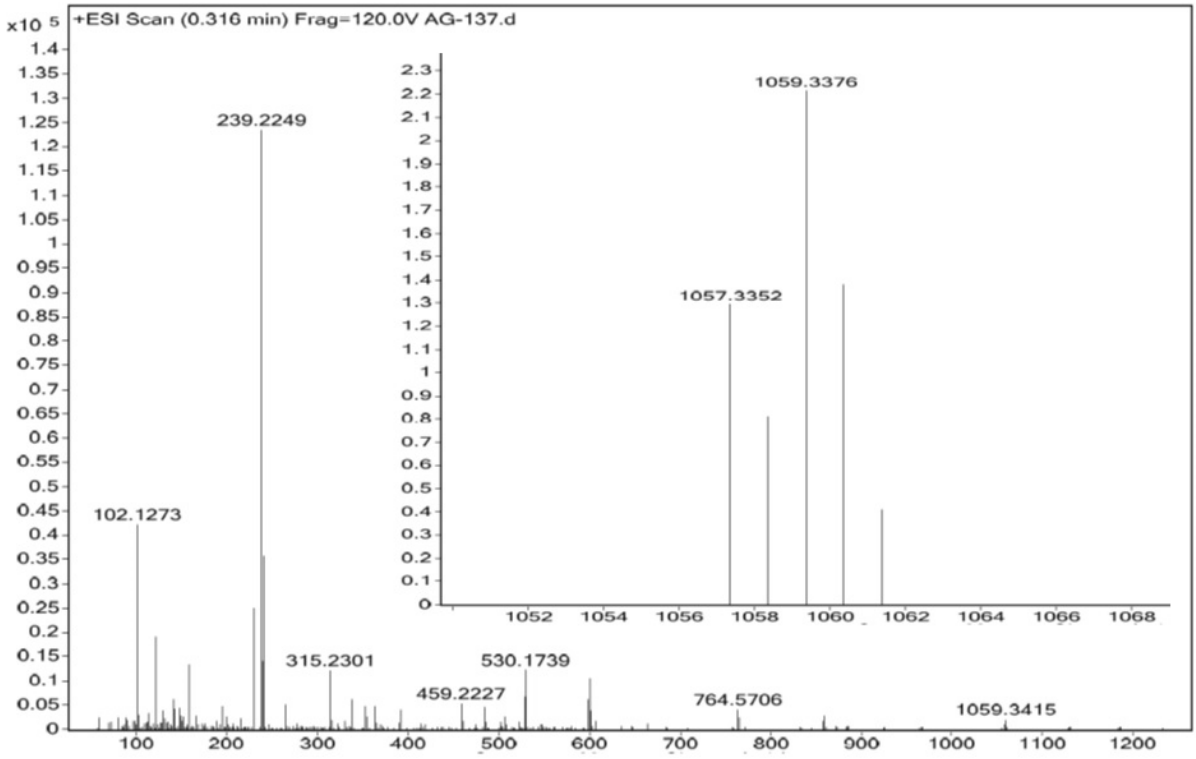

Fig. S6 Mass spectrum of **2** in DCM/MeOH showing the peak at 1059.3415 (*m/z*) assignable to $[M]^+$ at 298K.

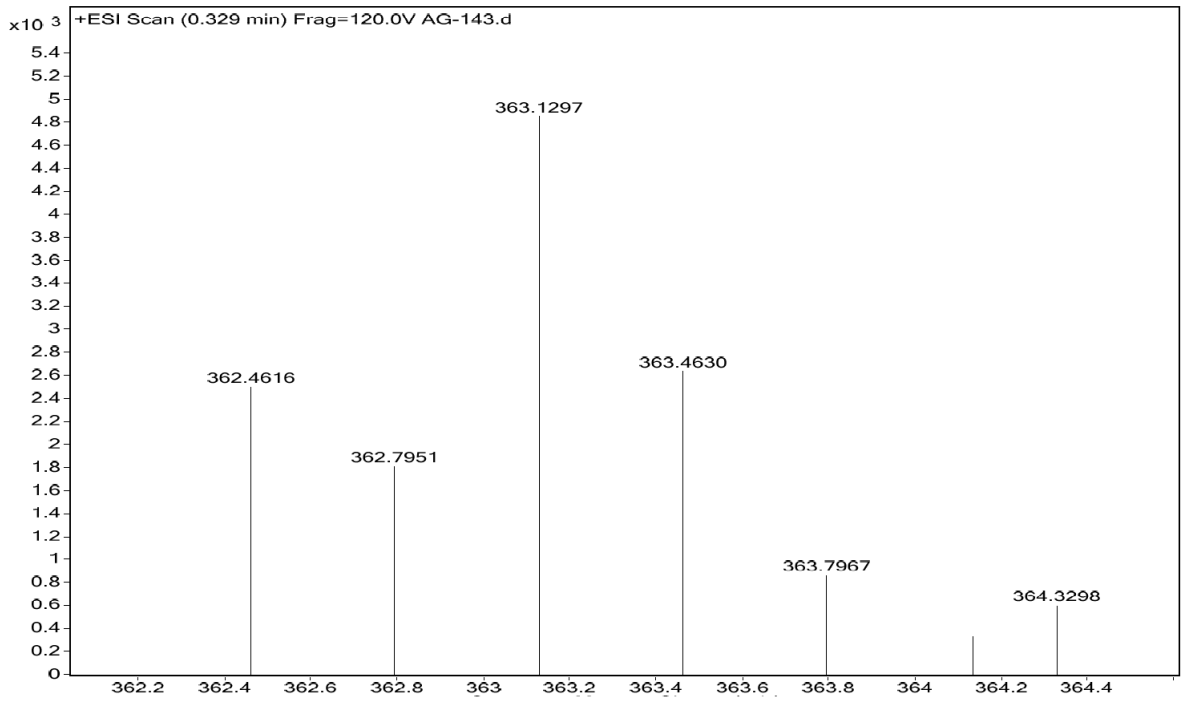

Fig. S7 Mass spectrum of **Ir1** in DCM/MeOH showing the peak at 363.1297 (*m/z*) assignable to $[M]^{3+}$ at 298K.

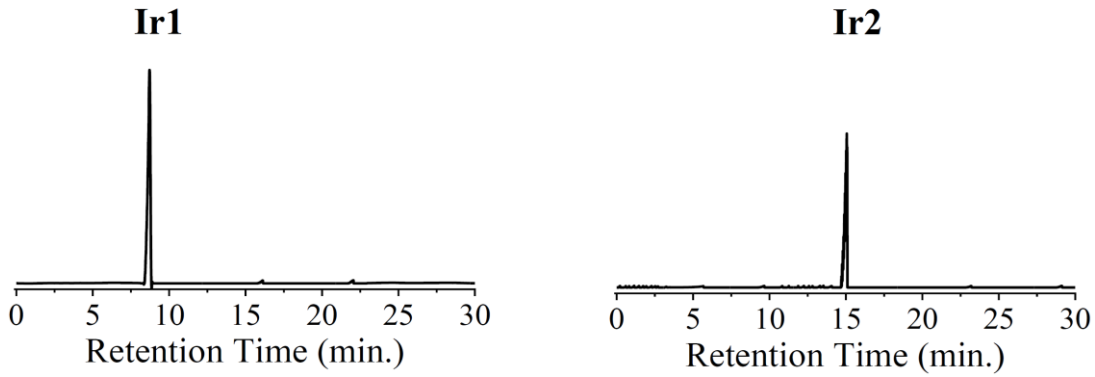

Fig. S8 HPLC chromatograms of **Ir1** and **Ir2** are showing the purity of the probes.

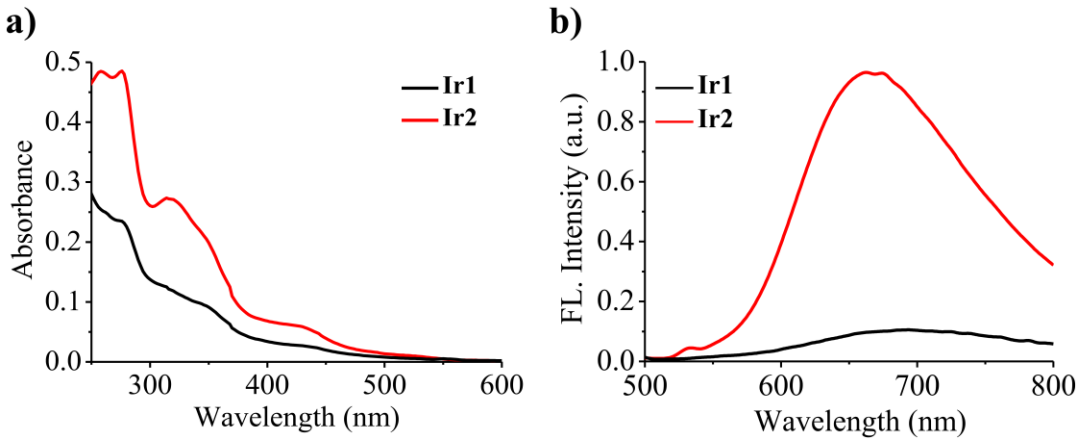

Fig. S9 (a) Absorption (10 μM) and (b) normalized emission (50 μM) spectra of the probes (**Ir1** and **Ir2**) were recorded in water at RT containing 0.2% and 1% DMSO, respectively. The emission spectra were measured upon excitation at 425 nm.

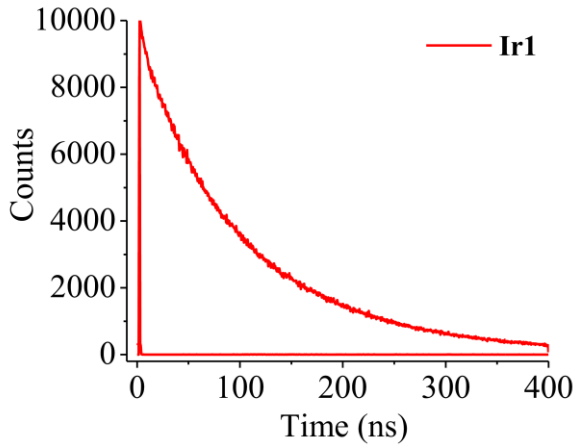

Fig. S10 Emission decay curve for the probe **Ir1** in air-saturated MeCN at room temperature.

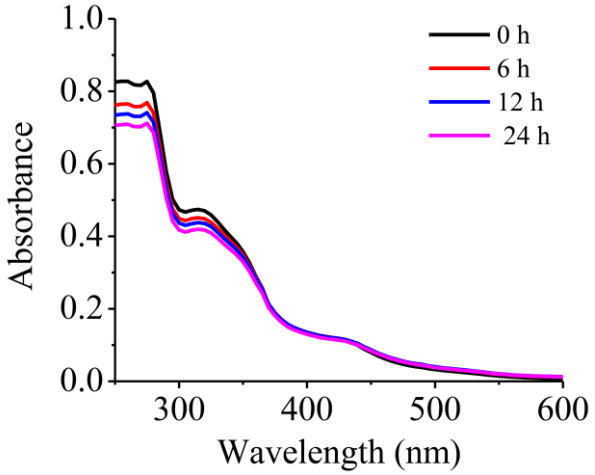

Fig. S11 Stability of the probe **Ir1** in PBS at room temperature up to 24 h.

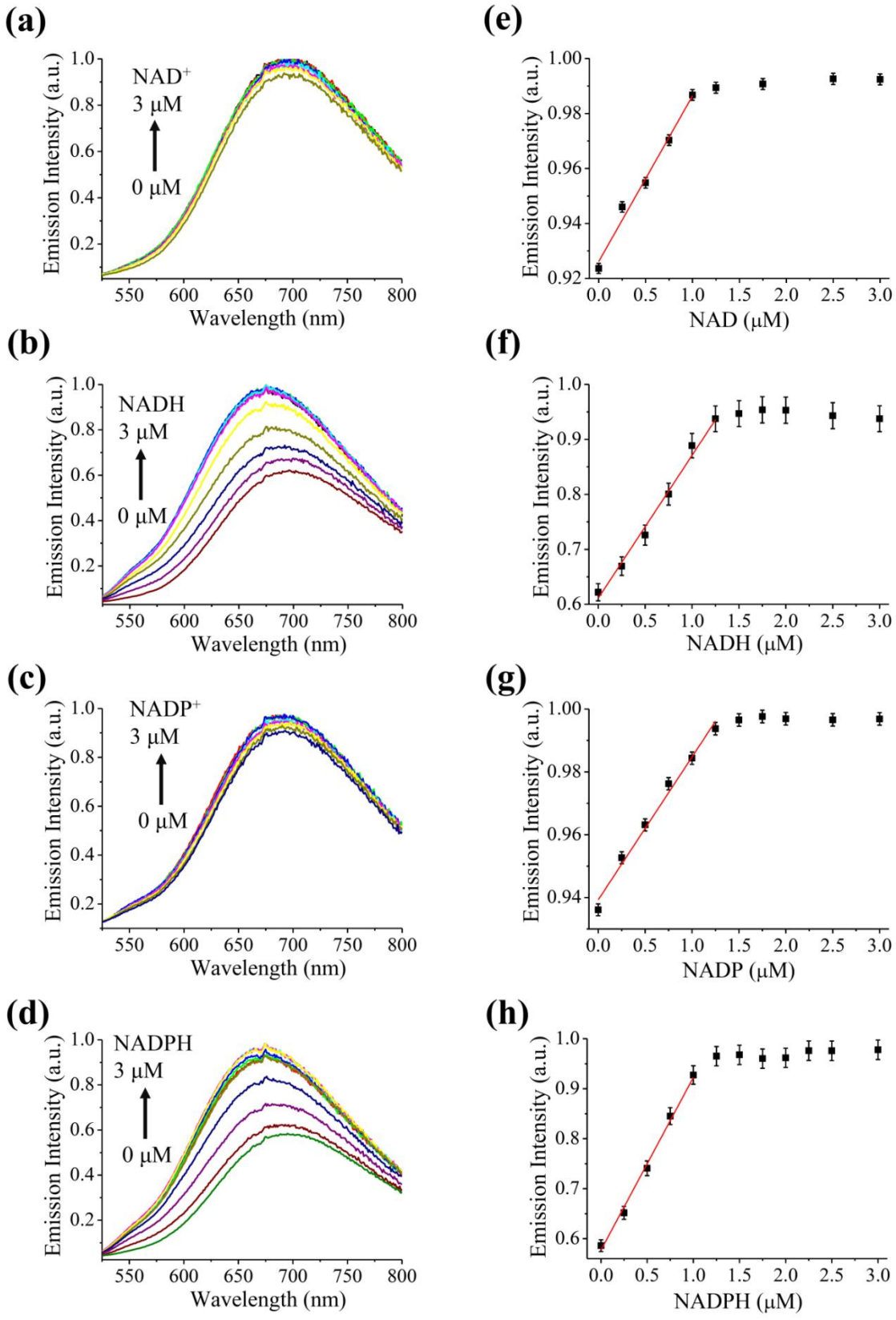

Fig. S12 (a-d) The titration spectra of **Ir1** (50 μM) upon gradual addition of NAD^+, NADH, $NADP^+$, and NADPH from 0 to 3 μM in aqueous medium, respectively. (e-h) Linear-fit curve of luminescence intensity of **Ir1** at 692 nm as a function of NAD species.

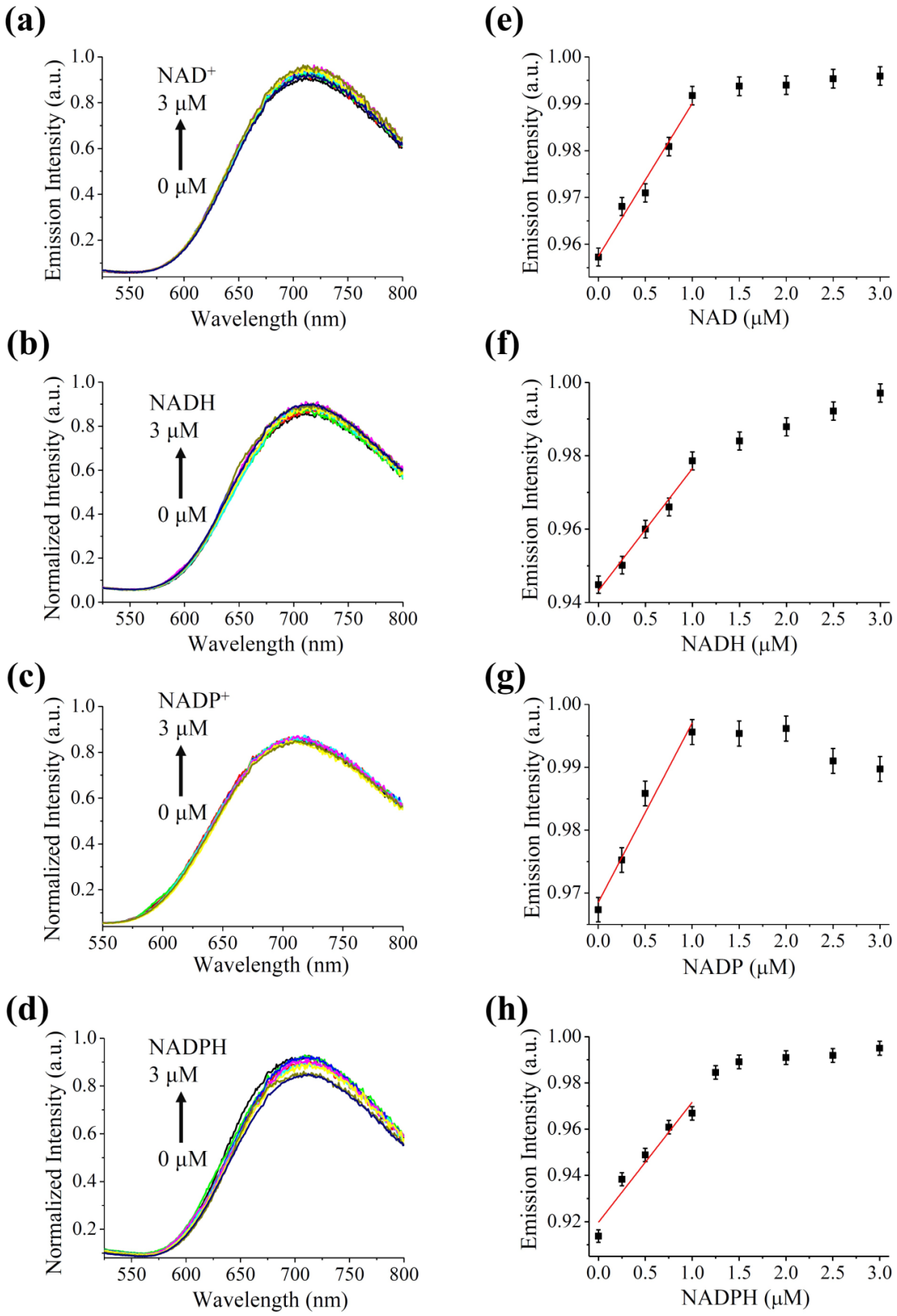

Fig. S13 (a-d) The titration spectra of **Ir2** (50 μM) upon gradual addition of NAD^+, NADH, $NADP^+$, and NADPH from 0 to 3 μM in aqueous medium, respectively. (e-h) Linear-fit curve of luminescence intensity of **Ir2** at 680 nm as a function of NAD species.

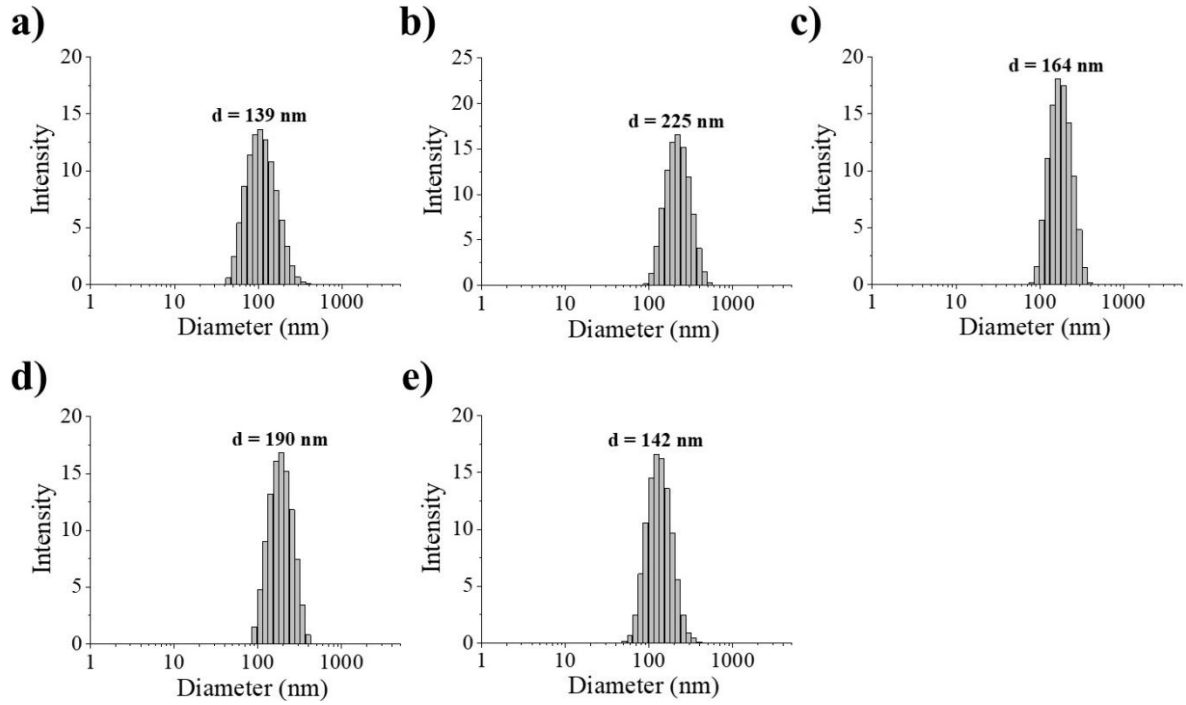

Fig. S14. Size distribution of probe **Ir1** (50 μM) in aqueous media (a) only probe, and (b-e) in the presence of 3 μM of NADPH, $NADP^+$, NADH, and NAD^+, respectively.

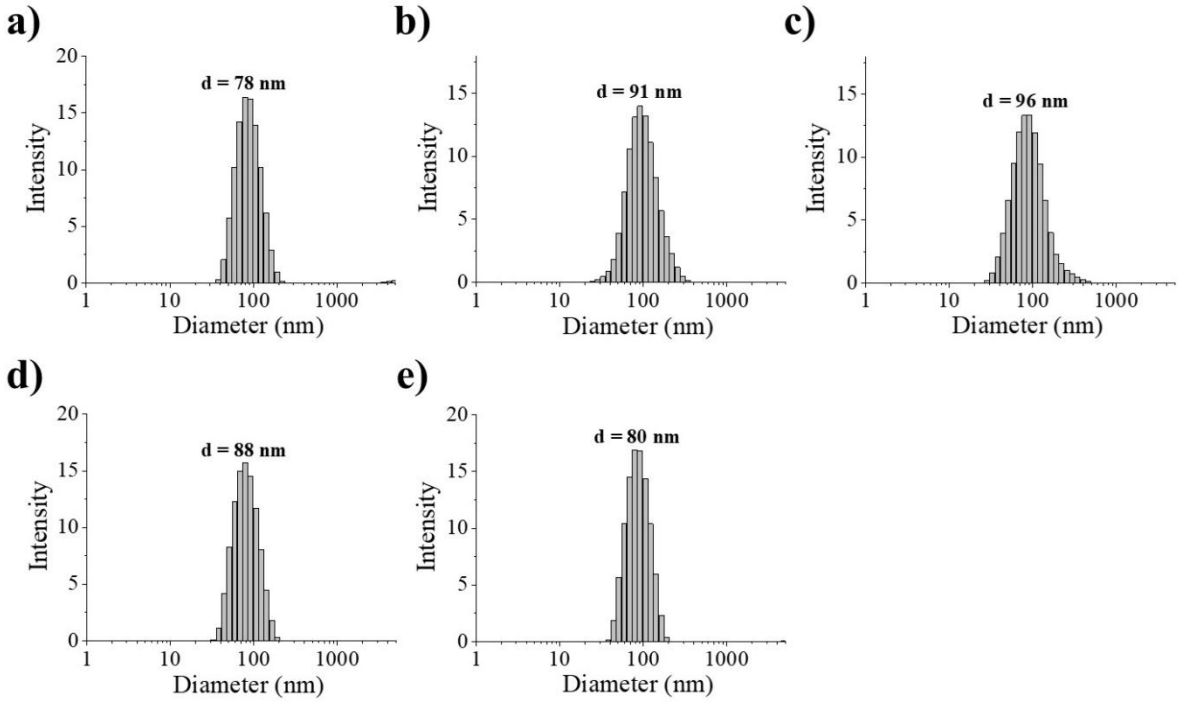

Fig. S15 Size distribution of probe **Ir2** (50 μM) in aqueous media (a) only probe, and (b-e) in the presence of 3 μM of NADPH, $NADP^+$, NADH, and NAD^+, respectively.

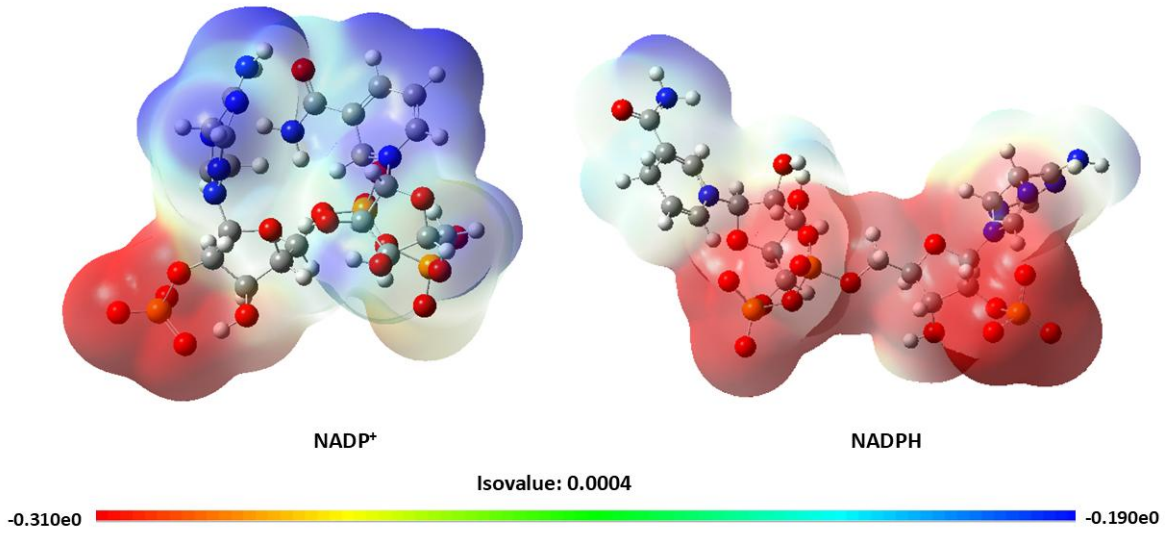

Fig. S16 ESP maps of **NADP**$^+$ and **NADPH**. The contours are colour-coded from red (electron rich) to blue (electron deficient).

The ground state geometry optimization of the structures of $NADP^+$ (having a positively charged pyridine nitrogen) and NADPH were performed using the DFT/B3LYP method with a 6-311G (d, p) basis set in the gas phase.

The 3D electrostatic surface potential (ESP) distribution of both $NADP^+$ and NADPH was mapped following energy calculations using the same basis set and functionals. In the case of the $NADP^+$ molecule which has a total charge of -3, a highly electron-deficient region is present over the positively charged pyridine ring, while one of the negatively charged phosphate groups exhibits a slight negative charge density. Additionally, this molecule adopts a closed structural conformation. In contrast, the NADPH molecule, which carries a net charge of -4, adopts an open structure, with a highly electron-rich region localized over all the negatively charged phosphate groups. Therefore, a comparison of the ESP shows that $NADP^+$ is more electron-deficient than NADPH.

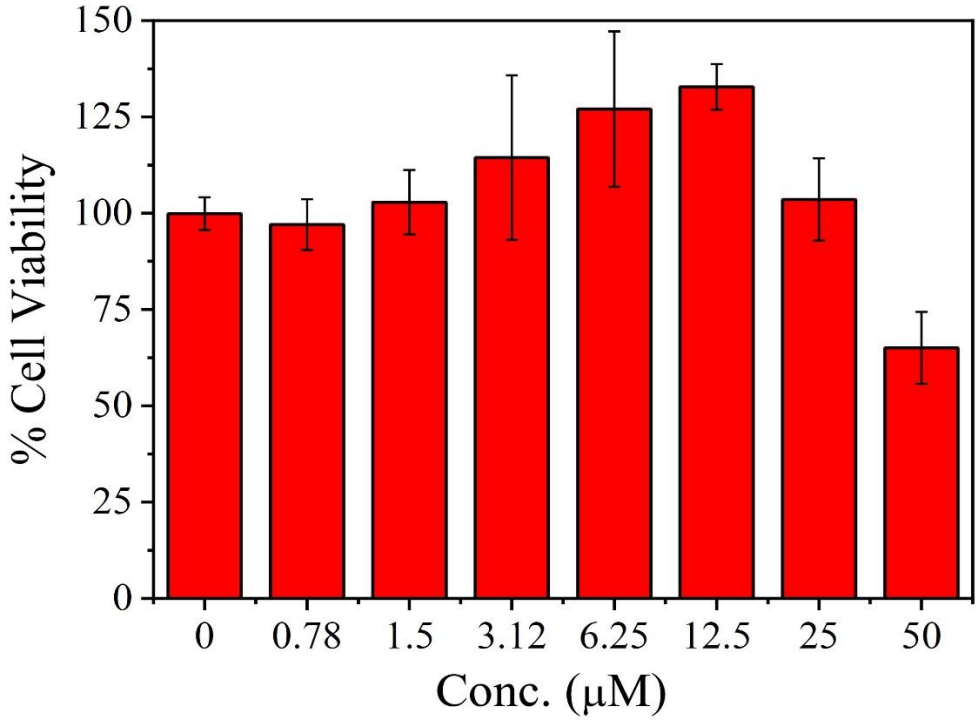

Fig. S17 Cell viability of MCF7 cells was assessed by the MTT assay following 24 h incubation with **Ir1**.

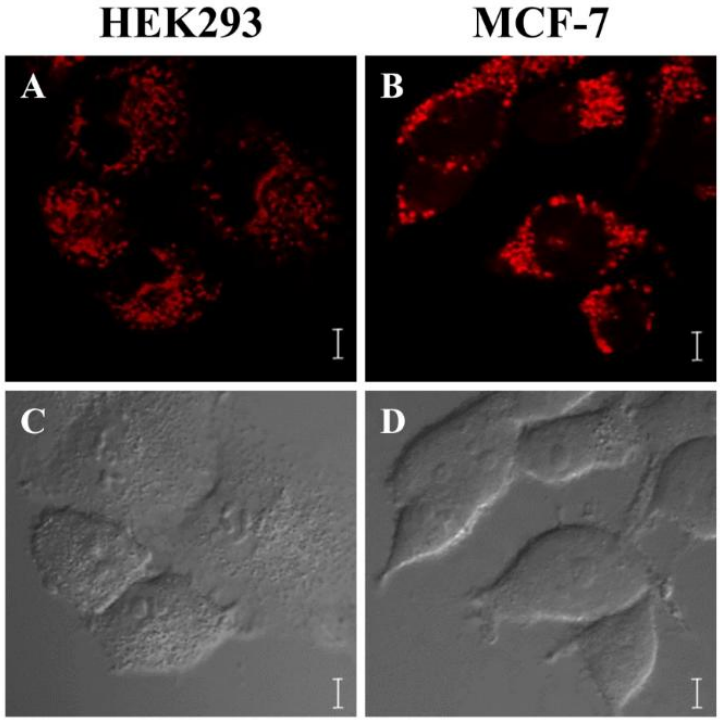

Fig. S18 NAD(P)H imaging in non-cancer (HEK293) and cancer (MCF7) cells. Fluorescence (A,B) and bright-field (C,D) images of HEK293 and MCF7 cells incubated with **Ir1** (10 μM) for 30 min. Cell images were acquired with red channel. Scale bar: 10 μm.

Supplementary References

1. A. Gautam, A. Gupta, P. Prasad and P. K. Sasmal, *Dalton Trans.*, 2023, **52**, 7843–7853.
2. A. Gupta, P. Prasad, S. Gupta and P. K. Sasmal, *ACS Appl. Mater. Interfaces*, 2020, **12**, 35967–35976.
3. G. Kumari, A. Gupta, R. Sah, A. Gautam, M. Saini, A. Gupta, A. Kushawaha, S. Singh and P. K. Sasmal, *Adv. Healthcare Mater.*, 2023, **12**, 2202411.
4. G. Jiang, J. Wang, Y. Yang, G. Zhang, Y. Liu, H. Lin, G. Zhang, Y. Li, and X. Fan, *Biosens. Bioelectron*., 2016, **85**, 62−67.